17th World Conference on Earthquake Engineering, 17WCEE
Sendai, Japan - September 13th to 18th 2020

AN ANALYTICAL METHOD OF BURIED STEEL PIPELINES AT STRIKE-SLIP FAULT CROSSINGS CONSIDERING PIPE OVALIZATION

C. Huang [1], W. Liu [2]

[1] *Ph.D candidate, Department of Structural Engineering, Tongji University, Shanghai, China,1710718@tongji.edu.cn*
[2] *Associate professor, Department of Structural Engineering, Tongji University, Shanghai, China, liuw@tongji.edu.cn*

Abstract

Buried pipe networks, such as gas and water networks, are always severely damaged during a strong earthquake, especially as the pipeline cross the fault zone. Existing analytical methods for buried steel pipelines at strike-slip fault crossings are aimed at the maximum strain of the pipeline, but the actual failure mode of the pipeline is not only tensile failure. The analytical method proposed in this paper takes into account the pipe ovalization and local buckling. It employs equations of equilibrium and compatibility of displacements to derive the axial force applied on the pipeline and adopts a combination of beam-on-elastic foundation and elastic-beam theory to calculate the developing bending moment. Then, the deformation of each cross-section is solved according to the combination of bending moment and lateral soil pressure, thus deriving the ovalization of each cross-section. The cross-section is assumed elliptical, and the ovalization is added to the iteration to get the true pipe strains. The failure mode of the pipe is judged by comparing the maximum ovalization, maximum strain and minimum strain.

Keywords: strike-slip faulting; strain; ovalization; local buckling;

1. Introduction

Buried pipe networks are always severely damaged during a strong earthquake, especially as the pipeline cross the fault zone. In previous earthquakes, such as the San Fernando earthquake (1971), the Izmit earthquake in Turkey (1999), the Chi-Chi earthquake (1999), the buried steel pipelines at active fault crossings were severely damaged. Up to now, three kinds of approaches are developed to address the pipeline behavior under strike-slip faults, including analytical methods, finite element methods and experimental methods. The analytical methods can provide an approximate and fast solution so some of which are adopted by design codes.

After the earthquake in San Fernando in 1971, the seismic response analysis of buried pipelines crossing the fault zone attracted the attention of scholars. The initial analytical method was proposed by Newmark and Hall [1], using a simplified analytical model of a long cable with small displacements, and consequently adopted by the ASCE guidelines [2] for the seismic design of pipelines. Kennedy et al. [3] extended the pioneering work of Newmark and Hall [1], by taking into account soil-pipeline interaction in the transverse. Wang et al. [4] made further improvements to simplify the deformed pipeline as a bending large deformation beam with single curvature and an elastic foundation beam. Then, non-linear stress and strain distribution on the pipeline cross-section and the unfavorable contribution of axial force to bending stiffness are considered [5-7].

Existing analytical methods for buried steel pipelines at strike-slip fault crossings are aimed at the maximum strain of the pipeline, but the actual failure mode of the pipeline is not only tensile failure. This paper proposes an analytical method for buried steel pipelines at strike-slip fault crossings considering pipe ovalization and pipe buckling. The remaining parts of this paper are organized as follows. Section 2 introduces the solution steps of this analytical method; then, the influences of pipe diameter and fault angle are discussed in Section 3. Conclusions are given in Section 4.

2. Solution steps

The analytical method presented in this paper extends the analytical methodology originally proposed by Karamitros et al [7]. The maximum axial force and bending moment of the pipeline are calculated according to the previous method, and the analysis model is shown in Fig. 1. However, when solving the ovalization of each section, the lateral force of the soil along section AB is assumed no longer uniformly distributed. The ovalization of each section is composed of two parts: caused by the lateral force of soil and by the pipe bending. Next, the ovalization is added to the iteration process to get the true pipe strains. Finally, the failure mode is determined: buckling dominant, axial tensile dominant or ovalization dominant.

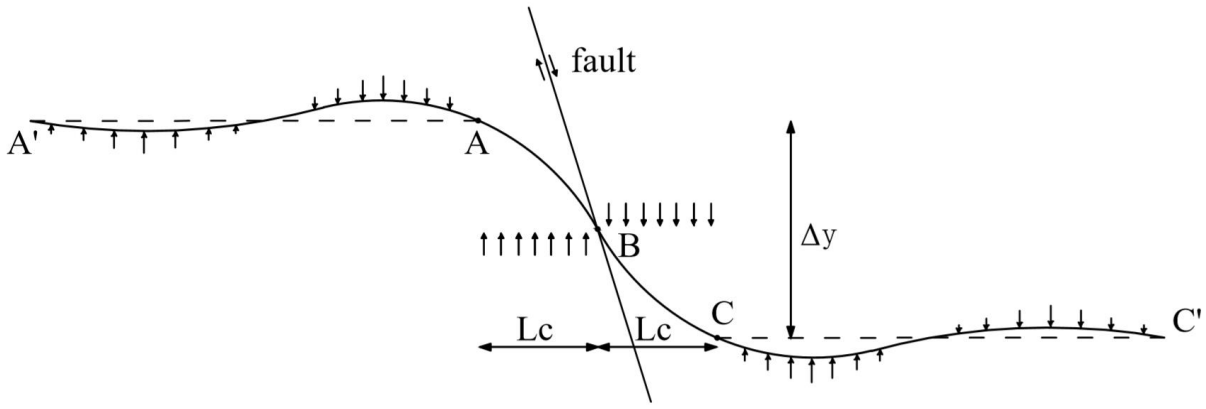

Fig. 1 Pipeline analysis model

2.1 The maximum bending moment and axial force

According to previous researches [4], the differential equilibrium equation for the elastic line of segment A'A (Fig. 1) is

$$E_1 I_0 w'''' + kw = 0 \tag{1}$$

where E_1 is the elastic Young's modulus of the pipeline steel, I_0 is the moment of inertia of the circle section, k is the elastic constant of the transverse horizontal soil springs. Herein, the cross section of segment A'A is assumed to circle section.

The elastic-beam theory is applicate in the line of segment AB, and the maximum bending moment can be calculated as [7]:

$$M_{\max} = V_B x_{max} - \frac{q_u x_{max}^2}{2} \tag{2}$$

where

$$V_B = \frac{24EI'\delta C_r + 12EI' q_u L_c^3 + 3 q_u C_r L_c^4}{24EI' L_c^2 + 8 C_r L_c^3} \tag{3}$$

$$x_{max} = \frac{V_B}{q_u} \tag{4}$$

where q_u is limit stress for transverse soil springs, E is the elastic Young's modulus of segment AB, I' is the moment of inertia of the elliptical section, L_c is pipeline unanchored length, $C_r = 2\lambda E_1 I_0$. Herein, the cross section of segment AB is assumed to elliptical section.

The maximum bending strain can be calculated as [7]:

$$\frac{1}{\varepsilon^b} = \frac{1}{\varepsilon_b^I} + \frac{1}{\varepsilon_b^{II}} = \frac{2EI'}{M_{\max} \cdot D} + \frac{2F_a}{q_u D} \tag{5}$$

where

$$F_a = \sigma_a A_s' \tag{6}$$

$$\sigma_a = \begin{cases} \sqrt{\frac{E_1 t_u \Delta x}{A_s'}} & \Delta x < \frac{\sigma_1^2 A_s}{E_1 t_u} \\ \frac{\sigma_1 (E_1 - E_2) + \sqrt{\sigma_1^2 (E_2^2 - E_1 E_2) + E_1^2 E_2 \Delta x \frac{t_u}{A_s'}}}{E_1} & \Delta x > \frac{\sigma_1^2 A_s}{E_1 t_u} \end{cases} \tag{7}$$

where t_u is limit soil-pipeline friction force, Δx is fault displacement, parallel to the pipeline longitudinal axis. A_s' is the area of the elliptical section. E_2 is the plastic Young's modulus of the pipeline steel.

2.2 Solution of the ovalization parameter

The ovalization of each section is composed of two parts: caused by the lateral force of soil and by the pipe bending. The specific algorithms are given below:

2.2.1 Caused by lateral force of soil

Pipeline of segment AB is simplified to an analysis model shown in Fig. 2 (a). In order to meet the load balance of each section, that is, the lateral force of the soil and the pipe shear force are equal, it is assumed that the shear force is distributed to each small segment area. According to the thin-walled circular pipe shear flow distribution rule, the shear stress at the neutral plane is $\tau_{max} = \frac{2q_{uc}}{\pi}$, and the shear stess at the farthest point from the neutral plane is 0 (Fig. 2 (b)). Herein, $\tau_\theta = \frac{2q_{uc}}{\pi}\left(1 - \frac{\theta}{\pi/2}\right)$.

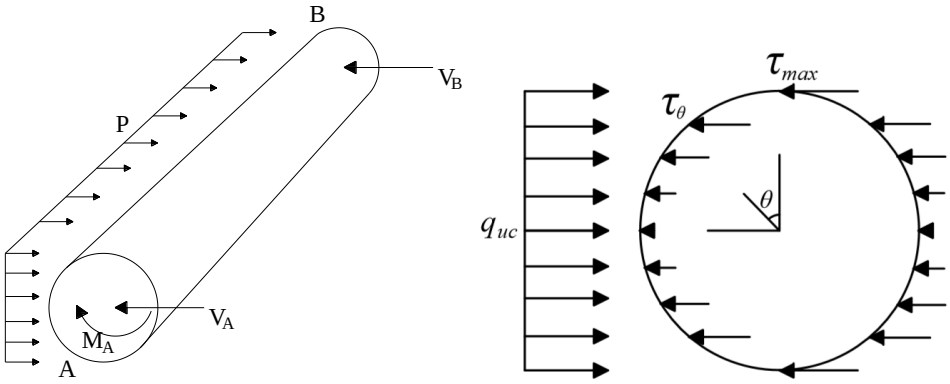

(a) (b)

Fig. 2 Analysis model for pipeline segment AB

The analysis model of Fig. 2 (b) can be can be partitioned into two parts, as shown in Fig. 3, and the ring deflection can be derived by adding the deformations of the two structures.

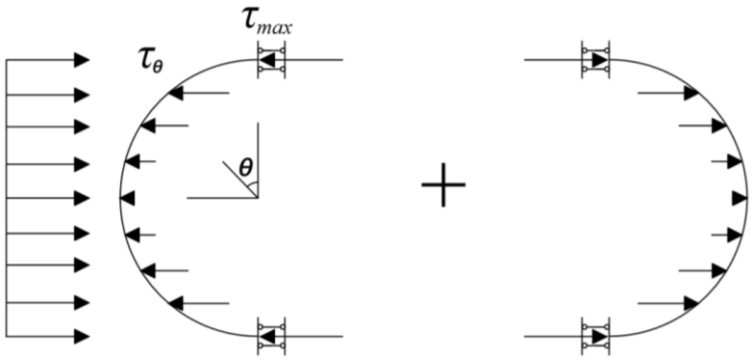

(a) (b)

Fig. 3 Partitioning of the pipe cross section into two parts

Application of elastic theory yields the deflection along the direction of shear:

$$\Delta 1 = \Delta L + \Delta R = \frac{0.0833 q_{uc} \cdot R^4}{E I_t} \tag{8}$$

where R=D/2, $I_t = \frac{t^3}{12}$, t is the pipeline thickness, $q_{uc} = q_u \cdot 1/D$.

Note that there will be a certain distance (x_{max}) between point B and the pipeline section of the most unfavorable combination of axial and bending strains. The lateral displacement of the pipe section at this position is assumed to:

$$\Delta y' = \frac{\Delta y}{2} \cdot \left(1 - sin\left(\frac{x_{max}}{L_c} \cdot \frac{\pi}{2}\right)\right) \tag{9}$$

The lateral soil force is approximately assumed to:

$$q_{lateral} = \begin{cases} q_u \cdot \frac{\Delta y'}{y_u} & \Delta y' < y_u \\ q_u & \Delta y' \geq y_u \end{cases} \tag{10}$$

where y_u is the pipe-soil lateral yield displacement.

2.2.2 Caused by pipe bending

The cross section of the pipeline will undergo rotational deformation when the pipeline is bent. The axial compressive stress σ_c and axial tensile stress σ_t will generate stress components q_c and q_t perpendicular to the pipeline, as shown in Fig. 4 [8]. The stress components will deform the pipe section.

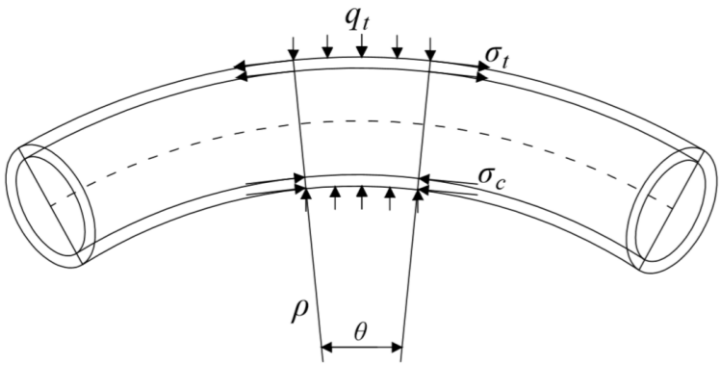

Fig. 4 Ovalization mechanism of the pipe cross section

According to the balance equation and geometric equation, elliptical stress can be derived as:

$$q_i = \frac{\sigma_i t}{\rho} \ (i = c, t) \tag{11}$$

where $\rho = \frac{D}{2 \cdot \varepsilon^b}$. therefore:

$$q_i = \frac{2\sigma_i t \varepsilon^b}{D} \ (i = c, t) \tag{12}$$

The force diagram of the pipeline cross section can be expressed as Fig. 5. Herein, the angles $\theta_{1,2}$ define the portion of the cross-section that is under yield. For simplicity of calculation, the portion that not under yield are ignored. Morever, the axial compressive (tensile) stress σ_i is assumed to be σ_1. The bent pipe has a squeezing effect on the soil so that the soil will generate additional lateral force q'_{soil}, and the lateral forces is equal to: $q'_{soil} = q_t \cdot \theta_1 - q_c \cdot \theta_2$.

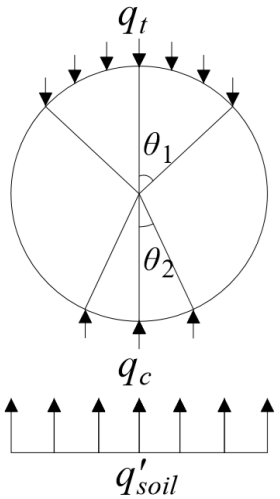

Fig. 5 The force diagram of the pipeline cross section

Similar to Fig. 2 (b). The analysis model of Fig. 5 can be partitioned into three parts and the ring deflection can be derived by adding the deformations of the three structures. Application of elastic theory yields the deflection caused by pipe bending:

$$\Delta 2 = \Delta D_{q_t} + \Delta D_{q_c} + \Delta D_{q'_{soil}} \tag{13}$$

$$\Delta D_{q_i} = \frac{q_i \cdot R^4}{EI_t}\left(-\frac{1}{4}\theta_i^2 + \frac{1}{8}cos2\theta_i + \frac{\pi}{4}\theta_i - cos\theta_i + \frac{2\theta_i cos\theta_i}{\pi} - \frac{4sin\theta_i}{\pi} + \frac{7}{8}\right) \tag{14}$$

$$\Delta D_{q'_{soil}} = \frac{0.0213 q'_{soil} \cdot R^4}{EI_t} \tag{15}$$

Finally, the total ring defletion can be calculated as:

$$\Delta D = \Delta 1 + \Delta 2 \tag{16}$$

The ovalization parameter can be calculated as:

$$\Delta f = \frac{\Delta D}{D} \tag{17}$$

Note that the value of $\theta_{1,2}$ will be given in section 2.3.

2.3 Solution of the axial strain

Existing methodologies [5-7] calculate the axial strain considering non-linear stress and strain distribution on the circle cross section. Elliptical cross section is considered in this paper (Fig. 6).

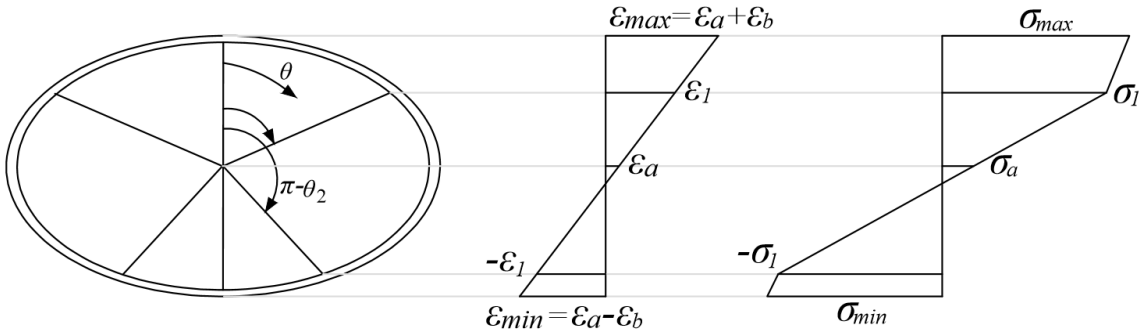

Fig. 6 Non-linear stress and strain distribution on the elliptical pipeline cross-section

The strain distribution on the cross-section is written as:

$$\varepsilon = \varepsilon_a + \varepsilon_b cos\theta \tag{18}$$

The corresponding distribution of stresses on the pipeline cross-section is given by:

$$\sigma = \begin{cases} \sigma_1 + E_2(\varepsilon - \varepsilon_1) & 0 \le \theta < \theta_1 \\ E_1\varepsilon & \theta_1 \le \theta \le \pi - \theta_2 \\ -\sigma_1 + E_2(\varepsilon + \varepsilon_1) & \pi - \theta_2 < \theta \le \pi \end{cases} \tag{19}$$

where

$$\theta_{1,2} = \begin{cases} \pi & \frac{\varepsilon_1 \mp \varepsilon_a}{\varepsilon_b} < -1 \\ arccos\left(\frac{\varepsilon_1 \mp \varepsilon_a}{\varepsilon_b}\right) & -1 \le \frac{\varepsilon_1 \mp \varepsilon_a}{\varepsilon_b} \le 1 \\ 0 & 1 < \frac{\varepsilon_1 \mp \varepsilon_a}{\varepsilon_b} \end{cases} \tag{20}$$

With the deformation of the pipeline section, the area and the moment of inertia of the pipeline cross-section change. As shown in Fig. 7, the area A'_s and the moment of inertia I' can be derived as follow:

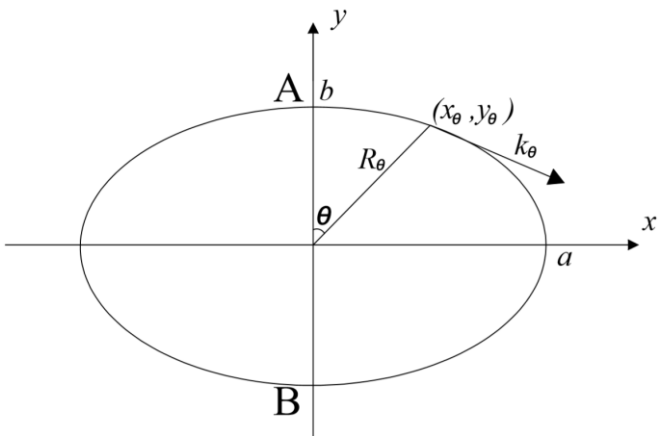

Fig. 7 Ellplical pipeline cross-section

The elliptic equation is:

$$\frac{x^2}{a^2}+\frac{y^2}{b^2}=1 \tag{21}$$

where $a=(1+f)\cdot\frac{D}{2}-\frac{t}{2}$, $b=(1-f)\cdot\frac{D}{2}-\frac{t}{2}$.

$$A_s'=2\int_A^B t\cdot ds=2\int_0^\pi t\cdot\sqrt{1+k_\theta^2}\cdot|dx|=2\int_0^\pi t\cdot\sqrt{1+k_\theta^2}\cdot\left|\frac{dx_\theta}{d\theta}\right|\cdot d\theta \tag{22}$$

$$I'=2\int_0^\pi y_\theta^2\cdot t\cdot\sqrt{1+k_\theta^2}\cdot\left|\frac{dx_\theta}{d\theta}\right|\cdot d\theta \tag{23}$$

where $k_\theta=-\frac{x_\theta}{y_\theta}\cdot\frac{b^2}{a^2}$, $\frac{dx_\theta}{d\theta}=\frac{R_\theta}{d\theta}\cdot sin\theta+R_\theta\cdot cos\theta$, $R_\theta=\sqrt{\frac{a^2b^2}{b^2sin^2\theta+a^2cos^2\theta}}$, $\frac{R_\theta}{d\theta}=\frac{1}{2}\cdot\frac{1}{R_\theta}\cdot\frac{a^2b^2(a^2-b^2)\cdot sin2\theta}{(b^2sin^2\theta+a^2cos^2\theta)^2}$

The axial force can be evaluated by the intergration over the elliptical cross-section:

$$\begin{aligned}F_a&=2\int_A^B\sigma\cdot t\cdot ds=2\int_0^\pi\sigma\cdot t\cdot\sqrt{1+k_\theta^2}\cdot|dx|=2\int_0^\pi\sigma\cdot t\cdot\sqrt{1+k_\theta^2}\cdot\left|\frac{dx_\theta}{d\theta}\right|\cdot d\theta\\&=2\int_0^{\theta_1}[\sigma_1+E_2(\varepsilon-\varepsilon_1)]\cdot t\cdot\sqrt{1+k_\theta^2}\cdot\left|\frac{dx_\theta}{d\theta}\right|\cdot d\theta\\&+2\int_{\theta_1}^{\pi-\theta_2}E_1\varepsilon\cdot t\cdot\sqrt{1+k_\theta^2}\cdot\left|\frac{dx_\theta}{d\theta}\right|\cdot d\theta\\&+2\int_{\pi-\theta_2}^{\pi}[-\sigma_1+E_2(\varepsilon+\varepsilon_1)]\cdot t\cdot\sqrt{1+k_\theta^2}\cdot\left|\frac{dx_\theta}{d\theta}\right|\cdot d\theta\end{aligned} \tag{24}$$

The axial strain can be evaluated using the equilibrium condition between the applied axial force (Eq. (6)) and the one obtained from Eq. (24).

2.4 Iteration of Young's modulus and ovalization

Using the already defined stress distribution on the pipeline cross-section, the corresponding bending moment can be calculated using Eq. (25)

$$M_{max} = 2\int_A^B R_\theta \cdot cos\theta \cdot \sigma \cdot t \cdot ds$$
$$= 2\int_0^{\theta_1} R_\theta \cdot cos\theta \cdot [\sigma_1 + E_2(\varepsilon - \varepsilon_1)\,] \cdot t \cdot \sqrt{1 + k_\theta^2} \cdot \left|\frac{dx_\theta}{d\theta}\right| \cdot d\theta$$
$$+ 2\int_{\theta_1}^{\pi-\theta_2} R_\theta \cdot cos\theta \cdot E_1\varepsilon \cdot t \cdot \sqrt{1 + k_\theta^2} \cdot \left|\frac{dx_\theta}{d\theta}\right| \cdot d\theta$$
$$+ 2\int_{\pi-\theta_2}^{\pi} R_\theta \cdot cos\theta \cdot [-\sigma_1 + E_2(\varepsilon + \varepsilon_1)] \cdot t \cdot \sqrt{1 + k_\theta^2} \cdot \left|\frac{dx_\theta}{d\theta}\right| \cdot d\theta \tag{25}$$

Therefore, the secant modulus for the next iteration can be calculated as:

$$E'_{sec} = \frac{M_{max}D}{2I'\varepsilon_b^I} = \frac{M_{max}D}{2I'}\left(\frac{1}{\varepsilon^b} - \frac{1}{\varepsilon_b^{II}}\right) \tag{26}$$

In Section 2.2, the value of bending strain is needed to solve the ovalization parameter, so an initial value of the ovalization should be assumed before calculating, and step 2.1-2.4 are repeated, until convergence is accomplished.

2.5 Judgement of failure modes

Three failure modes are considered in this paper: tensile failure, pipe buckling failure and excessive ovalization failure.

· Longitudinal tensile strain limit of 3%, as recommended within the Eurocode [9].

· Excessive ovalization of the pipeline cross-section characterized by the critical ovalization parameter is assumed equal to 15% [10].

· According to ABS guideline [11], which takes into account the effects of pipe ovalization, the compressive strain should satisfy Eq. (27)

$$\frac{\varepsilon}{\varepsilon_b} + \frac{p_e - p_i}{p_c} \le g(f) \tag{27}$$

3. Case study

3.1 Results compared with Karamitros' [7]

The maximum strain of the pipeline was studied in Karamitros' work. Fig. 8(a) shows the comparison between analytical predictions of maximum strain, axial strain and bending strain using the method proposed in this paper and in reference [7]. Fig. 8(b) shows relationship between maximum ovalization parameter of the pipeline and fault displacement. The angle formed by the fault trace and the pipeline axis β is 60° and the corresponding pipeline parameters are listed in Tab. 1. The limit stress for transverse soil springs and the limit soil-pipeline friction force are given by ASCE [12].

Tab. 1 Pipe size and steel properties

Outer diameter (m)	Wall thickness (m)	Buried depth (m)	Elastic Young's modulus (E_1)	Plastic Young's modulus (E_2)	Yield stress (σ_1)	Failure stress (σ_2)
0.9144	0.0119	4	210GPa	1.088GPa	490MPa	531MPa

(a)

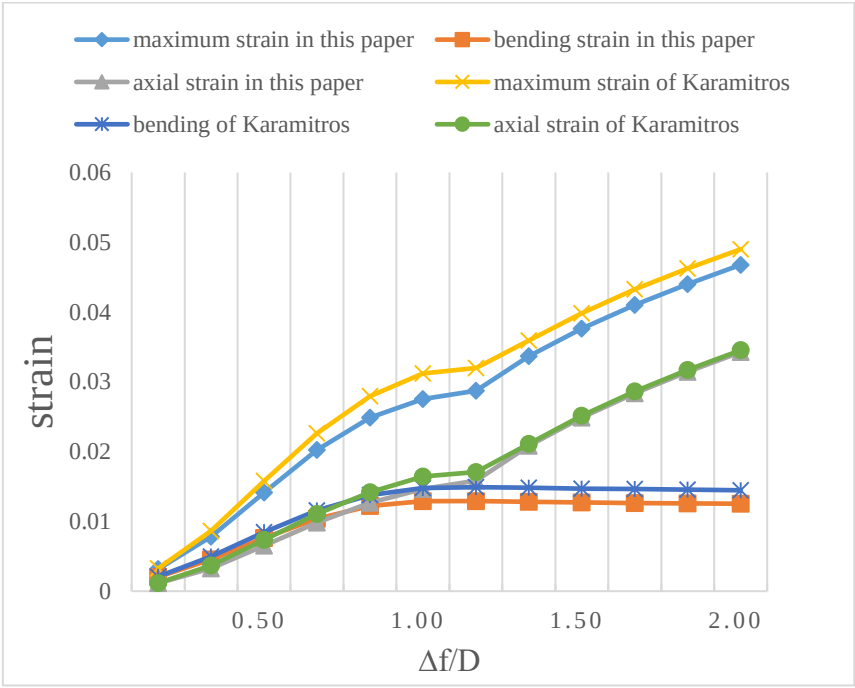

(b)

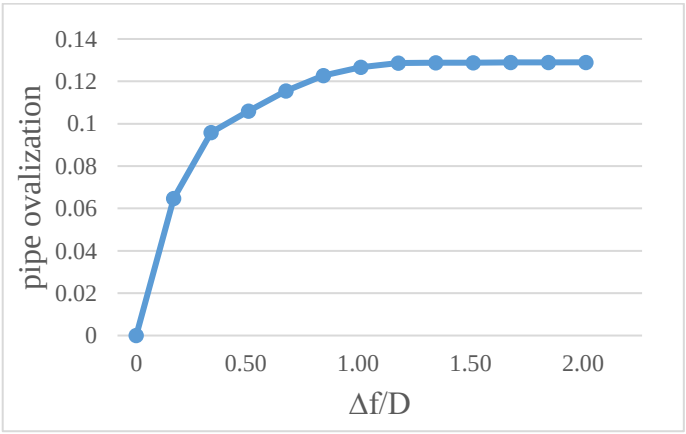

Fig. 8 Pipeline performance at strike-slip faults ($\beta = 60°$)

From Fig. 8(a), when the ovalization of the pipeline is taken into account, the maximum strain and bending strain decrease slightly, while the axial strain remain basically unchanged. Fig. 8(b) shows that the ovalization of the pipeline increases with the increase of the fault displacement, but in the region of large displacements, the bending strain of the pipeline and the lateral force of the soil basically remain unchanged, resulting that the pipe ovalization also tends to be stable.

3.2 Effects of pipe diameter and crossing angle β

Two pipe diameters are adopted and the corresponding parameters are listed in Tab. 2. For these two steel pipes, the limit fault displacements corresponding to each crossing angle are summarized in graphical form in Fig. 9.

Tab. 2 Pipe size and steel properties

Outer diameter (m)	Wall thickness (m)	Buried depth (m)	Elastic Young's modulus (E_1)	Plastic Young's modulus (E_2)	Yield stress (σ_1)	Failure stress (σ_2)

0.325	0.0055	1	210GPa	1.088GPa	490MPa	531MPa
3	0.03	8	210GPa	1.088GPa	490MPa	531MPa

(a)

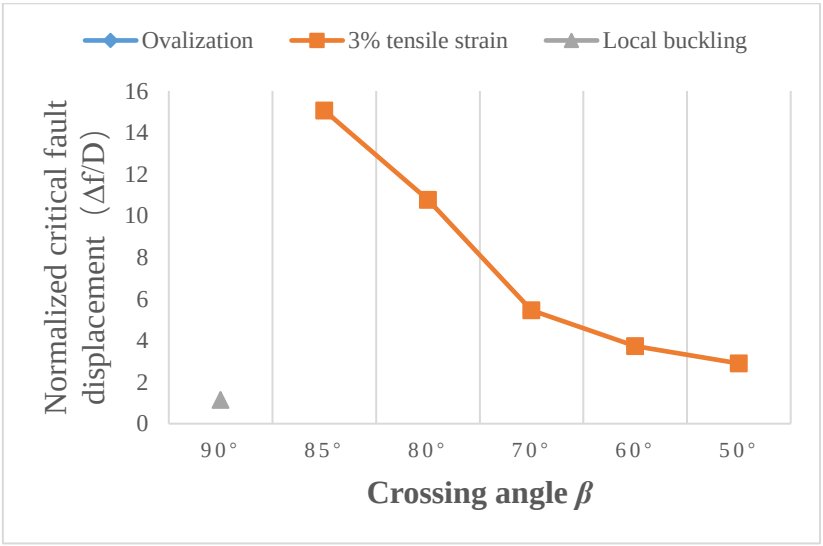

(b)

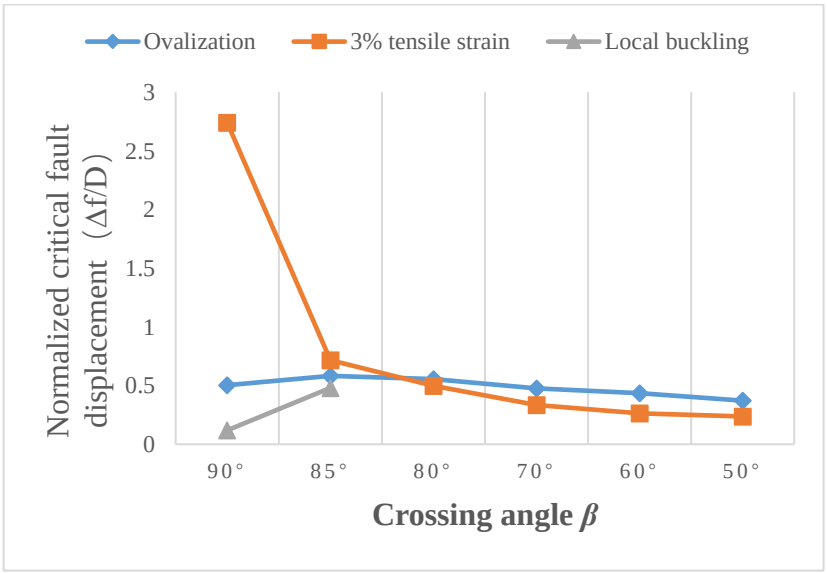

Fig. 9 Normalized critical fault displacement for various performance limits at different angles of β ((a) D=0.325m, (b) D=3m)

For a small-diameter pipeline, Fig. 9 (a) indicates that tensile failure is the dominant limit state, and the ovalization of the pipeline is small. However, as shown in Fig. 9 (b), large-diameter pipelines, which have a large diameter-thickness ratio and buried depth, will undergo large cross-section deformation when crossing faults, and the failure form is not just tensile failure. When β is close to 90 °, buckling failure and excessive ovalization are the dominant limit states; and when β is smaller, tensile failure is the dominant limit state.

4. Conclusion

This paper proposes an analytical method for pipeline crossing strike-slip faults. Compared with existing methods, pipe ovalization and pipe buckling are taken into account in this method proposed this paper. The pipeline cross-section is assumed elliptical to derive the pipeline response, which is more consistent with the

actual situation. In order to illustrate above methods, several cases are studied. Results show that both pipe diameter and crossing angle have a certain effect on pipeline performance; for large-diameter pipeline, buckling failure and excessive ovalization can be the dominant limit states; and the pipe generally has the largest normalized critical fault displacement when the crossing angle is close to 80°.

5. Copyrights

6. References

[1] Newmark NM, Hall WJ (1975): Pipeline design to resist large fault displacement: *Proceedings of US national conference on earthquake engineering*. 1975: 416-425.

[2] ASCE (1984): Guidelines for the seismic design of oil and gas pipeline systems: *Committee on Gas and Liquid Fuel Lifelines. American Society of Civil Engineers, New York*, 473.

[3] Kennedy RP, Chow AM, Williamson RA (1977): Fault movement effects on buried oil pipeline. *Transportation engineering journal of the American Society of Civil Engineers*, 103(5): 617-633.

[4] Wang LRL, Yeh YH (1985): A refined seismic analysis and design of buried pipeline for fault movement. *Earthq. Eng. Struct. Dyn*, 13(1): 75-96.

[5] Karamitros DK, Bouckovalas GD, Kouretzis GP (2011): An analytical method for strength verification of buried steel pipelines at normal fault crossings. *Soil Dyn. Earthq. Eng*, 31(11): 1452-1464.

[6] Trifonov OV, Cherniy VP (2010): A semi-analytical approach to a nonlinear stress–strain analysis of buried steel pipelines crossing active faults. Soil Dynamics and Earthquake Engineering, 30(11): 1298-1308.

[7] Karamitros, D.K., G.D. Bouckovalas, and G.P. Kouretzis, Stress analysis of buried steel pipelines at strike-slip fault crossings. *Soil Dyn. Earthq. Eng*, 2007. 27(3): 200-211.

[8] Wang HP, Li X, Zhou J (2017): Analytical solution of ultimate bending moment bearing capacity of pipeline considering ellipticity and material anisotropy. *Ocean. Eng*, 35 (01): 71-79. [In Chinese]

[9] Eurocode CEN. 8 (2004): Design of structures for earthquake resistance. Part, 1: 1998-1.

[10] Gresnigt AM (1987): Plastic design of buried steel pipelines in settlement areas.

[11] Guide ABS (2006): Guide for building and classing subsea riser systems. *American Bureau of Shipping, Houston*: 37-39.

[12] Alliance AL (2001): Guidelines for the design of buried steel pipe: *American Society of Civil Engineers*.

